ChemPubSoc Europe

DOI: 10.1002/cplu.201402153

Synthesis of Bright Alkenyl-1*H*-1,2,4-triazoles: A Theoretical and Photophysical Study

Cristina Cebrián,*[a, b, d] Juan de Mata Muñoz,[a] Cristian Alejandro Strassert,[c] Pilar Prieto,[a] Ángel Díaz-Ortiz,*[a] Luisa De Cola,[b] and Antonio de la Hoz[a]

A sustainable synthesis of alkenyl-1*H*-1,2,4-triazoles through the Hiyama reaction is reported, which employs water as solvent and sodium hydroxide to activate the silyl group under microwave irradiation, thereby leading to high product yields (51–93%) in very short reaction times. Two substitution patterns were attained owing to the different reactivity of the third and fifth positions of the 1*H*-1,2,4-triazole unit, as evidenced by calculated condensed Fukui functions. Moreover, all compounds are good blue emitters (Φ_F up to 0.69) in THF solution, although they exhibit an optical behavior dependent on the substitution. Excited-state theoretical investigations by the configuration interaction singles method and time-dependent density functional theory were performed not only to support and elucidate the studied photophysical properties, but also to create a predictive model to reduce the cost and optimize the search for new blue emitters based on this class of alkenyl-1*H*-1,2,4-triazoles.

Introduction

Photoactive molecules that contain a heterocyclic moiety have proven to be important materials for advanced optoelectronic applications including optical information processing, photovoltaic cells, photodynamic therapy, and others.[1] The 1,2,4-triazole moiety is an important system that is present in a large number of compounds with a wide variety of uses in many fields, such as medicinal chemistry,[2] materials science,[3] and organocatalysis.[4] Compounds based on this heterocyclic motif are appealing owing to their high electron affinity and thermal stability, as well as their diverse coordination modes. As a result, there are numerous examples in the literature of materials bearing 1,2,4-triazole moieties, such as transition-metal complexes,[5] metal–organic frameworks,[6] and polymers,[7] all of which exhibit interesting luminescence properties among other features. More interestingly, 1,2,4-triazole rings tend to decrease the effective π conjugation of aromatic systems,[7b,8] thus facilitating the design of blue emitters. Nonetheless, detailed reports concerning the luminescence properties of small molecules that incorporate this heterocyclic unit are rare.[9]

The majority of the routes for the synthesis of 1,2,4-triazoles rely on intramolecular condensation reactions.[10] Additionally, halogenated 1,2,4-triazoles can be modified by nucleophilic substitution reactions,[11] and also through coupling protocols such as Suzuki–Miyaura-type,[12] Stille-type,[13] Heck-type,[14] or Ullmann-type[15] reactions.

Regardless of the selected synthetic route, special attention should be paid to the sustainability of the overall process. Within the paradigm of "green chemistry",[16] the development of sustainable and environmentally friendly synthetic approaches of tailored materials is favored. The strategies for the achievement of such processes are mainly focused on the use of alternative solvents, as well as improved energy efficiencies and yields.[17] The establishment of the relationship between structure and properties is also of fundamental importance to avoid unnecessary synthetic steps. In this sense, the use of computational studies has become essential as these can be considered as the "greenest" experiments, which allow the selection of potentially interesting molecules.[18]

For the computation of luminescence properties, the possibility of simulating emission spectra has been reported.[19] The main difficulty in performing such studies concerns the determination of the excited-state geometry because of the limited range of theories with available analytic derivatives.[20] The simplest approach is the ab initio configuration interaction with all singly excited determinants (configuration interaction singles, CIS)[21] method, which provides a cost-effective, semiquantita-

[a] Dr. C. Cebrián, Dr. J. de Mata Muñoz, Dr. P. Prieto, Prof. Á. Díaz-Ortiz, Prof. A. de la Hoz
Departamento de Química Inorgánica, Orgánica y Bioquímica
Facultad de Ciencias Químicas, Universidad de Castilla–La Mancha
Avenida Camilo José Cela s/n, 13071 Ciudad Real (Spain)
Fax: (+34) 926-295318
E-mail: Angel.Diaz@uclm.es

[b] Dr. C. Cebrián, Prof. L. De Cola
Institut de Science et d'Ingénierie Supramoléculaires (ISIS)
Université de Strasbourg
8 Alleé Gaspard Monge, 67083 Strasbourg (France)

[c] Dr. C. A. Strassert
Physikalisches Institut and Center for Nanotechnology (CeNTech)
Universität Münster
Heisenbergstrasse 11, 48149 Münster (Germany)

[d] Dr. C. Cebrián
Current address:
Institut de Chimie, Physique et Matériaux (ICPM)
Université de Lorraine, 1 Boulevard François Aragó, 57070 Metz (France)
E-mail: cristina.cebrian-avila@univ-lorraine.fr

Supporting information for this article is available on the WWW under http://dx.doi.org/10.1002/cplu.201402153.

tive way to study excited states. The main drawback of this method is the accuracy, which is comparable to that of the Hartree–Fock (HF) method for the ground state, owing to the limited treatment of correlation effects. Therefore, even though the excited-state potential energy surfaces can be fairly good, the excitation energies are largely overestimated. In an effort to improve these computed energies beyond HF quality, time-dependent density functional theory (TD-DFT)[22] can be used. This approach includes the electron correlation and provides satisfactory results for both organic and organometallic compounds.[19,23]

Our group has been interested in the investigation of environmentally friendly processes that involve microwave irradiation as the energy source.[24] We have also implemented theoretical studies to rationalize the effects of conventional heating and microwave irradiation on the reaction mechanisms.[25] Recently, we described a new method to prepare alkenyl-1*H*-1,2,4-triazole derivatives by a Heck reaction.[14] However, this synthetic procedure leads to product mixtures with tedious purification processes and moderate yields. In the current context of sustainable synthesis, palladium-catalyzed cross-coupling reactions of organosilicon compounds with organic halides (Hiyama reaction)[26] have become fairly popular from an environmental point of view in comparison with other more polluting processes. Silicon-derived compounds are very attractive owing to their stability, low cost, and accessibility, which also make them suitable for industrial purposes.[27] Herein, we report on the preparation of π-conjugated alkenyl-1*H*-1,2,4-triazoles by means of the Hiyama reaction in conjunction with microwave radiation as the energy source. The photophysical properties of the final compounds were investigated extensively. Furthermore, we assessed the use of computational calculations to validate this approach for the design of new triazole-based photoactive materials.

Results and Discussion

Synthesis of the dialkenyl-1*H*-1,2,4-triazoles

In the last decade, several microwave-assisted Hiyama cross-coupling reactions have been reported.[28] In this context, we employed a protocol that avoids fluoride anions to activate the organosilicon derivative and employs hydroxide anions in water and microwave irradiation as energy source.[28c] To study the scope of this reaction on a 1*H*-1,2,4-triazole moiety, we performed the coupling between the dihalo-substituted compound **1** and several arylvinyltriethoxysilanes (**2**) with slightly modified reaction conditions (Scheme 1). In most cases, only monosubstituted 1*H*-1,2,4-triazoles **3** were obtained in acceptable to good yields (58–85%; Table 1). The reaction appears to work similarly with siloxanes containing either electron-withdrawing or electron-donating groups. More energetic reaction conditions (time or temperature) or an increase in the siloxane/triazole ratio to obtain higher yields or disubstituted products led to intractable reaction mixtures for which isolation of pure products in acceptable yields was very difficult. The low reactivity of the 1*H*-1,2,4-triazole on its 3-position (see below),

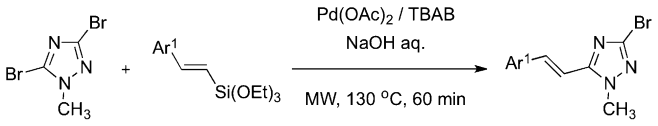

1 2 3

Scheme 1. C–C cross-coupling reactions of 3,5-dibromo-1-methyl-1*H*-1,2,4-triazole (**1**) with arylvinyltriethoxysilanes **2**. TBAB = tetrabutylammonium bromide, MW = microwave.

Table 1. Preparation of 5-substituted alkenyl-1*H*-1,2,4-triazoles **3** and 3,5-disubstituted alkenyl-1*H*-1,2,4-triazoles **4** by Hiyama coupling under microwave irradiation.

Entry	Silane (Ar^1)	Silane (Ar^2)	**3** [%][a]	**4** [%][a]
1	**2a** $Ar^1 = C_6H_5$	–	**3a** (85)	–
2	**2b** $Ar^1 = p\text{-}CH_3O\text{-}C_6H_4$	–	**3b** (60)	–
3	**2c** $Ar^1 = p\text{-Ph-}C_6H_4$	–	**3c** (58)	–
4	**2d** Ar^1 = naphth-1-yl	–	**3d** (77)	–
5	**2e** $Ar^1 = p\text{-}F_3C\text{-}C_6H_4$	–	**3e** (80)	–
6	**2a** $Ar^1 = C_6H_5$	**2a** $Ar^2 = C_6H_5$	–	**4a** (71)
7	**2b** $Ar^1 = p\text{-}CH_3O\text{-}C_6H_4$	**2b** $Ar^2 = p\text{-}CH_3O\text{-}C_6H_4$	–	**4b** (93)
8	**2c** $Ar^1 = p\text{-Ph-}C_6H_4$	**2c** $Ar^2 = p\text{-Ph-}C_6H_4$	–	**4c** (51)
9	**2d** Ar^1 = naphth-1-yl	**2d** Ar^2 = naphth-1-yl	–	**4d** (67)
10	**2e** $Ar^1 = p\text{-}F_3C\text{-}C_6H_4$	**2b** $Ar^2 = p\text{-}CH_3O\text{-}C_6H_4$	–	**4e** (75)

[a] Product isolated by column chromatography on silica gel.

together with possible side reactions of the siloxane derivative[27] on increasing its concentration in the reaction mixture, might account for the unsuccessful efforts to obtain the disubstituted compounds in a single step.

To achieve the synthesis of the target disubstituted compounds **4**, a second cross-coupling reaction was performed on monosubstituted compounds **3** (Scheme 2). Interestingly, in this case 1*H*-1,2,4-triazoles **4** were obtained in good yields (51–93%; Table 1) without changing the reaction conditions. We tentatively explained this finding as being the result of a change in the reactivity of the C-3 position of the triazole ring. This hypothesis was subsequently confirmed by theoretical calculations (see below).

The *trans* configuration ($^3J_{H-H}$ ca. 16 Hz) of the double bonds in all of the compounds described herein was confirmed by

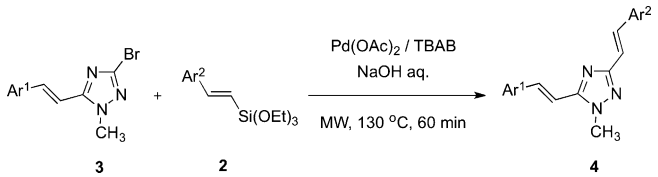

3 2 4

Scheme 2. C–C cross-coupling reactions of 5-alkenyl-3-bromo-1*H*-1,2,4-triazoles **3** with arylvinyltriethoxysilanes **2**.

^{1}H NMR spectroscopy. Therefore, this effective synthetic procedure provides simple access to a wide range of alkenyl-1*H*-1,2,4-triazole derivatives with different substitution patterns in a few minutes and with good yields.

Photophysical characterization

As a result of their potential interest as new chromophores, dialkenyl-1*H*-1,2,4-triazoles **4a–e** were selected and their photophysical properties were studied.

The UV/Vis absorption and emission spectra in solution are depicted in Figure 1 and Figures S1 and S2 in the Supporting Information, and the most meaningful photophysical data are summarized in Tables 2 and S1.

At room temperature in tetrahydrofuran (THF) solution, all compounds showed strong absorption bands ($\varepsilon = 2.0–3.1 \times 10^4\,M^{-1}cm^{-1}$) at high energies ascribed to π–π^* transitions. Upon excitation at 300 nm in air-equilibrated THF solution, all the compounds showed a featureless emission in the blue region of the spectrum. The effect of the different substitution patterns on the maximum emission wavelength ($\lambda_{em,max}$) was as follows: **4a** < **4b** < **4c** < **4d** < **4e**. The increase in the π system on going from phenyl to naphthyl to biphenyl substituents led to a bathochromic shift in the emission wavelength. For the phenyl-based derivatives (**4a–c,e**), the replacement of the *p*-H of the phenyl moiety by other groups also led to bathochromic shifts. This effect is particularly evident for compound **4e**, which contains two different groups (one electron donor, $-CH_3O-C_6H_4$, and one electron acceptor, $-CF_3-C_6H_4$).

The emission quantum yields (Φ_F) were in the range 0.25–0.56, except for compound **4b**, which had a value of only 0.04. These values are comparable to those of commercial blue dyes such as disodium 4,4′-bis(2-sulfostyryl)biphenyl ($\Phi_F = 0.23$ in H_2O)[29a] and quinine sulfate dihydrate ($\Phi_F = 0.54$ in 0.1 M H_2SO_4 aqueous solution).[29b]

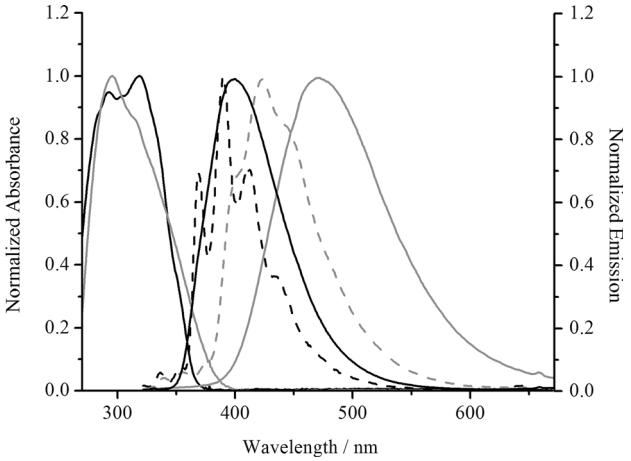

Figure 1. Room-temperature absorption (left) and emission spectra (right) for compounds **4a** (black) and **4e** (grey) in air-equilibrated THF solution (solid lines) and 77 K emission spectra (dashed lines) in 2-methyltetrahydrofuran (2-MeTHF) glassy matrices. $\lambda_{exc} = 300$ nm.

As far as the time-resolved measurements are concerned, the compounds showed biexponential decays in THF solution at room temperature, with characteristic fluorescence lifetimes of a few nanoseconds. In the case of compound **4b**, a monoexponential decay corresponding to a lifetime of 0.6 ns was obtained. The biexponential nature of the decays usually suggests the coexistence of several emissive species (owing to acid–base or conformational equilibria, aggregation processes, etc.) that affect the kinetics of the de-excitation process. Interactions with the solvent can also lead to complex decays.

Careful analysis of the emission spectra recorded at 77 K in 2-methyltetrahydrofuran (2-MeTHF) glassy matrices revealed the different character of the emission in both series of compounds. Compounds bearing the same substituent in both C-3 and C-5 positions of the triazole ring, namely **4a–d**, displayed

Table 2. Selected photophysical data for compounds **4a–d**.

Compound	Medium (*T* [K])	$\lambda_{abs,max}$ [nm] (ε [10^4 M^{-1}cm^{-1}])	$\lambda_{em,max}$ [nm][a]	Φ_F[b]	τ_{obs} [ns][c] (*A* %)[d]	k_r[e] [10^7 s^{-1}]	k_{nr}[f] [10^7 s^{-1}]
4a	THF (298)	293 (2.2), 318 (2.4)	397	0.56	1.84 (13), 2.94 (87)	22	17
	Tol (298)	318 (2.3)	394, 412 (sh)	0.28	1.79 (79), 2.77 (21)	14	35
	DMSO (298)	285 (2.4), 319 (2.1)	410	0.69	0.49 (23), 2.96 (74)	24	11
	2-MeTHF (77)	–	368, 388, 409, 432 (sh)	–	1.62 (62), 3.66 (36)	–	–
	PMMA 5 wt% (298)	–	399	0.24	0.66 (53), 2.35 (44)	–	–
4b	THF (298)	286 (3.1), 326 (2.6)	379 (sh), 405	0.04	0.60 (93)	–	–
	2-MeTHF (77)	–	377, 399, 421, 450 (sh)	–	1.94 (94)	–	–
4c	THF (298)	316 (2.2), 333 (2.2)	352 (sh), 390 (sh), 411	0.46	0.38 (20), 1.74 (80)	–	–
	2-MeTHF (77)	–	352, 372, 389, 412, 438, 468 (sh)	–	1.43 (96)	–	–
4d	THF (298)	328 (2.6)	365 (sh), 426	0.25	0.33 (20), 2.33 (70)	–	–
	2-MeTHF (77)	–	364, 402, 425, 450	–	2.35 (100)	–	–
4e	THF (298)	296 (2.4), 315 (2.0)	469	0.38	2.85 (13), 5.09 (87)	8	13
	Tol (298)	294 (3.4), 318 (2.7)	439	0.27	2.20 (15), 3.91 (85)	7	20
	DMSO (298)	288 (3.2), 318 (2.7)	525	0.23	3.22 (44), 4.62 (46)	6	19
	2-MeTHF (77)	–	397(sh), 420, 442(sh)	–	3.49 (97)	–	–
	PMMA 5 wt% (298)	–	435	0.51	0.91 (26), 3.90 (62), 7.48 (13)	–	–

[a] The abbreviation "sh" denotes shoulder. [b] Quantum yields were measured in an integrating sphere. $\lambda_{exc} = 300$ nm. [c] All the compounds were excited at $\lambda = 375$ nm. [d] Only lifetimes with $A > 10\%$ are shown. [e] The radiative rate constants were calculated by means of the equation: $k_r = \Phi_F/\tau_{obs}$. [f] The nonradiative rate constants were calculated by means of the equation: $k_{nr} = (1-\Phi_F)/\tau_{obs}$.

structured emissions with clear vibronic progressions and slight blueshifts of the emission maxima. Conversely, compound **4e** showed a smooth structured emission together with a remarkable hypsochromic shift (2488 cm^{-1}). Although **4a–d** emit from a rather apolar excited state that remains insensitive to the environment, **4e** possesses a lowest excited state with polar character and it is therefore fairly destabilized when solvent reorganization is prevented in such frozen matrices. In general, the decays became monoexponential and longer in comparison to those obtained at 77 K. Nevertheless, compound **4a** still exhibited a biexponential decay.

Complementary information about the character of the emitting excited state can be provided by performing solvent polarity-dependent (solvatochromism) emission studies. Compounds **4a** and **4e** were selected for these experiments as examples of the two observed behaviors for this class of chromophore. Hence, solvents of varying polarity—ranging from apolar toluene (Tol) to highly polar dimethyl sulfoxide (DMSO)—were chosen for the solvatochromism study. The solvatochromic fluorescence of both compounds is depicted in Figure S3, and the corresponding photophysical data are listed in Table S1. Compound **4a** showed slightly blueshifted emission maxima (900 cm^{-1}) upon decreasing the polarity of the solvent, which is consistent with the slight shift observed in frozen matrices. Nevertheless, the quantum yields did increase, reaching values up to 0.69 when DMSO was employed as solvent. The fluorescence decays were found to be biexponential for the three solvents. It is interesting to note the variation of the radiative and nonradiative constants, k_r and k_{nr}, on increasing the polarity of the surrounding media. A plausible explanation for this observation is that a higher-lying quenching state might be close in energy to the emitting one. For certain conformations and low polarities, this quenching state is close in energy and serves as a thermally accessible deactivation channel of the emissive state, a situation that explains both the higher contribution of the shorter component to the average lifetime and the lower quantum yield. As the polarity increases, the slight stabilization of the luminescent lowest excited state and a possible destabilization of the other state is enough to suppress this quenching effect. The larger energy gap also correlates with a larger radiative rate constant as the mixing of the emissive state with the dark state is diminished.

The structured emission at 77 K and the almost negligible solvatochromism suggest that the emitting state for equally substituted compounds **4a–d** is of the type π–π^*. The transitions take place in the same region of the molecule and, consequently, they are apolar in character. The quenching state could be of the type n–π^*, which is characteristic of heterocycles and is known to be much less efficient than the former ones. Moreover, this state would be of particular importance for **4b**, which has a quantum yield of 0.04, owing to the presence of two methoxy groups.

The behavior of compound **4e** differed markedly from that of **4a**. The emission of **4e** was clearly shifted to the red (3700 cm^{-1}) on increasing the polarity of the solvent. The quantum yields remained quite comparable (0.23–0.38), whereas the lifetimes were biexponential and the nonradiative rate constants one order of magnitude higher than the corresponding radiative ones in all solvents. In this case, and in contrast to **4a–d**, the less structured emission profile and the solvatochromism of compound **4e** indicate that its emission arises from an intramolecular charge-transfer state. The high polarity of this excited state makes it sensitive to the dielectric constant of the solvent and it constitutes a polarity sensor of the microenvironment.

Solid state

The good emission properties of the materials in fluid solutions prompted us to evaluate the emission of **4a** and **4e** in the solid state as thin films and as dispersions in a poly(methyl methacrylate) (PMMA) matrix. The emission spectra are shown in Figure S4 and the photophysical data are collected in Table S1. As shown in Figure S4, the solid-state emission of **4a** was in the blue region of the spectrum, as in solution, and the higher concentration in the thin films did not shift the emission maxima. The measured quantum yields were good (ca. 0.22) and were also independent of the doping concentration. With regard to **4e**, the emission maximum was bathochromically shifted towards the blue–green region with decreasing quantum yields (0.51–0.21 for 5 and 100 wt%, respectively) upon increasing the concentration of the chromophore, presumably because a higher doping rate also enhances the dielectric constant of the microenvironment within the polymer matrix.

Computational investigations

Chemical reactivity

Since Miethchen and co-workers[12a] reported the first cross-coupled compounds from halogenated 1*H*-1,2,4-triazole nucleosides, the different reactivity of the halogens located at positions C-3 and C-5 of the triazole ring has been demonstrated experimentally. The same preference has been found in the case of nucleophilic substitution reactions.[30] Houk and co-workers[31] studied the selectivity of palladium-catalyzed cross-coupling reactions of heterocycles substituted with identical halogen atoms. They concluded that the selectivity could be explained in terms of both bond dissociation energies and frontier molecular orbital interactions. Nonetheless, the Fukui theory is one of the most successful, simple, and best-known methods to assess the reactivity of the regions of a molecule.[32]

Therefore, in an attempt to rationalize the reactivity of the 1*H*-1,2,4-triazole, the condensed Fukui function for the nucleophilic attack (f_k^+)[33] was calculated at carbon atoms 3 and 5 of the triazole ring for compounds **1** and **3a** within the framework of DFT, by employing the functional PBE0 and 6-31+G(d,p) as basis set (Figure 2). The values are collected in Table S2. The different tendency towards the insertion of a nucleophilic fragment is clearly revealed and C-5 of the triazole **1** is the preferential site of attack (higher f_k^+). The negative value found for C-3 could explain the extremely low reactivity of this

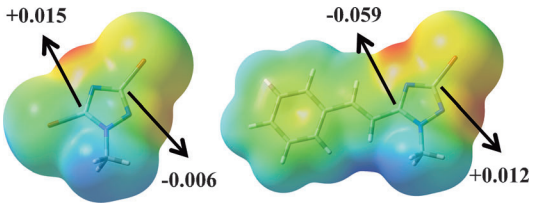

Figure 2. Electrostatic potential projected onto the electron density plots of **1** (left) and **3a** (right) at the PBE0/6-31+G(d,p) level of theory. The indicated values correspond to the respective condensed Fukui function for nucleophilic attack (f_k^+).

position for triazole **1** and the difficulty in obtaining dicoupled derivatives in a single reaction. The introduction of a styryl fragment at C-5 leads to complete inversion of the chemical reactivity between positions C-3 and C-5 of the triazole. It can be observed in compound **3a** that the electrophilicity of C-3 is enhanced after the coupling of styrene at C-5, whereas that of C-5 is markedly reduced. These results are consistent with the reactivity of this family of 1*H*-1,2,4-triazoles, and constitute a straightforward method to interpret the regioselectivity of the Hiyama reaction in this work.

Photophysical properties

A simulation of the experimental results was performed to predict the fluorescence emission of this class of materials. Geometrical parameters and electronic features of the molecules in their ground state (S_0) were studied by DFT, and computation of electronic transitions and singlet lowest-lying excited states (S_1) was performed by CIS and TD-DFT methods (see the Computational Details). At a first stage, the S_0 geometries of compounds **4a**–**e** were optimized at the PBE0/6-31G* level of theory (Figure 3). In molecules **4a**–**b** and **4e**, the triazole ring and the phenylvinyl units are almost within the same plane. However, the outer phenyl rings in **4c** deviate from planarity by about 37°. Compound **4d** has an even more distorted structure, with only the triazole and the vinylic units coplanar. To provide a pictorial representation of the ground-state electronic structure, the most relevant highest occupied molecular orbitals (HOMOs) and lowest unoccupied molecular orbitals (LUMOs) were calculated (Figure S5). A schematic representation of their energy levels is shown in Figure S6 and Table S3. The MOs are arranged in a similar manner for all compounds and they lie alternately on one half of the molecule. The extension of the π-conjugated system from **4a** to **4c** to **4d** leads to destabilization of both HOMO and LUMO. The introduction of groups with different electronic natures had the expected effect on the frontier orbitals: that is, electron donation on the HOMO raises the orbital energy, whereas electron withdrawal on the LUMO lowers it, and vice versa.

In an effort to shed light on the electronic transitions observed in the absorption spectra, the compounds were investigated at the TD-PBE0/6-311+G(2d,p) level. The computed vertical transitions were calculated at the equilibrium geometry of the corresponding S_0 state and are described in terms of the linear combination of one-electron excitations of molecular orbitals at that geometry (Table S4). The calculated vertical lowest energies mainly involved the HOMOs and LUMOs and represented the 0–0 transitions. The other vertical transitions

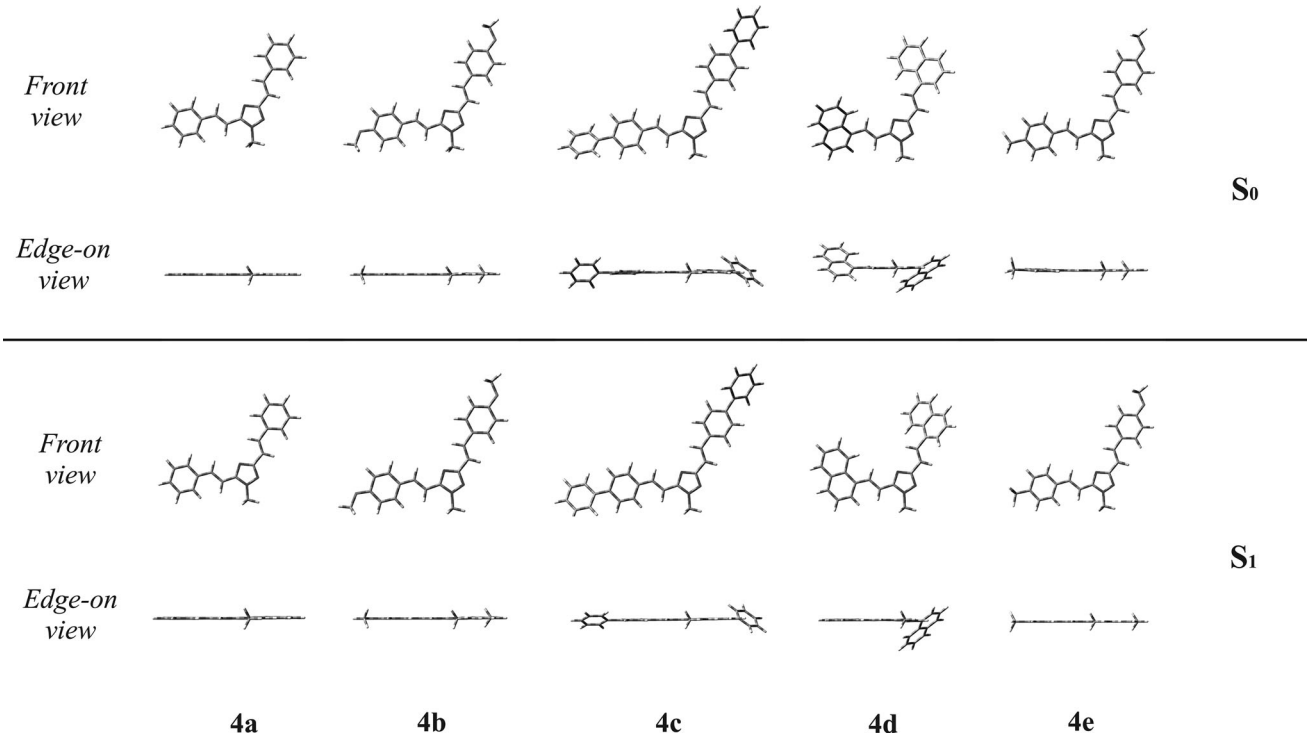

Figure 3. Front and edge-on views of optimized geometries of compounds **4a**–**e** in both the ground state (S_0) and the first singlet excited state (S_1).

agreed well with the absorption bands of the experimental spectra. Inspection of the MOs involved in the transitions showed that they are located in the same part of the molecule and comprise mainly HOMO−1, HOMO, LUMO, and LUMO+1. The orbitals can be described as π–π* in nature, which is in accordance with the high extinction coefficients calculated for these absorption bands.

Prior to the estimation of the fluorescence wavelengths, the geometry of the lowest singlet-manifold excited state must be optimized. This target was accomplished by employing the CIS method with the 6-31G* basis set. As it can be observed in Figure 3, all compounds undergo planarization upon excitation. This fact is particularly remarkable in **4d**, in which the naphthyl group on the C-5 substituent turns by 32° until it is aligned with the molecular plane. Further information was provided by the highest and lowest singly occupied molecular orbital (HSOMO and LSOMO, respectively) plots (Figure 4). In contrast to the ground-state frontier orbitals, SOMOs reflect the electronic situation after the geometrical reorganization of the molecule. Two distinct types of behavior can be observed for the compounds studied in this work. The SOMOs are displayed primarily on the substituent at C-5 of the triazole in the case of **4a**–**d**, that is, those with equivalent substituents. In contrast, each SOMO remains on a different half of the molecule for **4e**, which bears different substituents. Thus, it is possible to envisage the charge-transfer character of the emission of **4e**, in clear contrast to the localized charge reorganization of **4a**–**d**. This situation fully supports the conclusions of the experimental work (see above).

Additionally, analysis of the electronic density in the S_0 and S_1 states supports the previously described behavior (Figure S7). The dipole moment in compounds **4a**–**d** does not change significantly ($\Delta\mu \approx 0.65$ D) upon excitation since only the substituent at C-5 is ultimately involved in the emissive process. In contrast, the excitation in **4e** is followed by a reorganization of the electronic charge and this causes a notable increase in the dipole moment of the molecule ($\Delta\mu = 3.27$ D).

Despite succeeding in the structure optimization of molecules in their excited states, the CIS method usually overestimates the transition energies as it neglects electron correlation effects. The computed vertical emission transitions were determined using TD-PBE0/6-311+G(2d,p) in vacuum and THF, and the results are collected in Table S5 and Figure S8. To introduce a correction to the computational results, a statistical analysis (linear regression) was performed to improve the concordance between theory and experiment. An excellent linear correlation ($R^2 = 0.919$) was found between experimental ($E_{em,exp}$) and calculated ($E_{em,calc}$) emission energies in vacuum according to Equation (1):

$$E_{em,exp} = -0.624 + 1.227\,E_{em,calc} \quad (1)$$

The good fit of the data evidenced the validity of our approach and suggested that not only are the gas-phase calculations fully valid for estimating emission energies, but also that highly accurate predictions can be envisaged for structurally related derivatives.

In addition to CIS, we tried to extend our approach by also optimizing the excited-state structures with the TD-DFT approach as the analytical gradients for this method are also known. As an example, compounds **4a** and **4e** were optimized at the lowest singlet excited state at the TD-PBE0/6-31G* level of theory. Subsequent estimation of the emission energies was obtained as described previously with TD-PBE0/6-311+G(2d,p). The calculated energies were 2.85 and 2.41 eV for **4a** and **4e**,[34] respectively. These values led to errors that were one order of magnitude higher than the corresponding ones obtained by the CIS method. Therefore, this work clearly illustrates that more expensive calculations, such as optimization at the TD-DFT level, are not always the most appropriate choice.

Conclusion

We have reported the easy preparation of differently substituted alkenyl-1*H*-1,2,4-triazoles by the Hiyama reaction. These compounds have appealing photophysical properties and these have been thoroughly studied both experimentally and computationally. The methodology described herein involves the use of readily available, low-toxicity alkenylsiloxanes, water as the reaction solvent, and microwave irradiation as the energy source. The good yields obtained for this class of com-

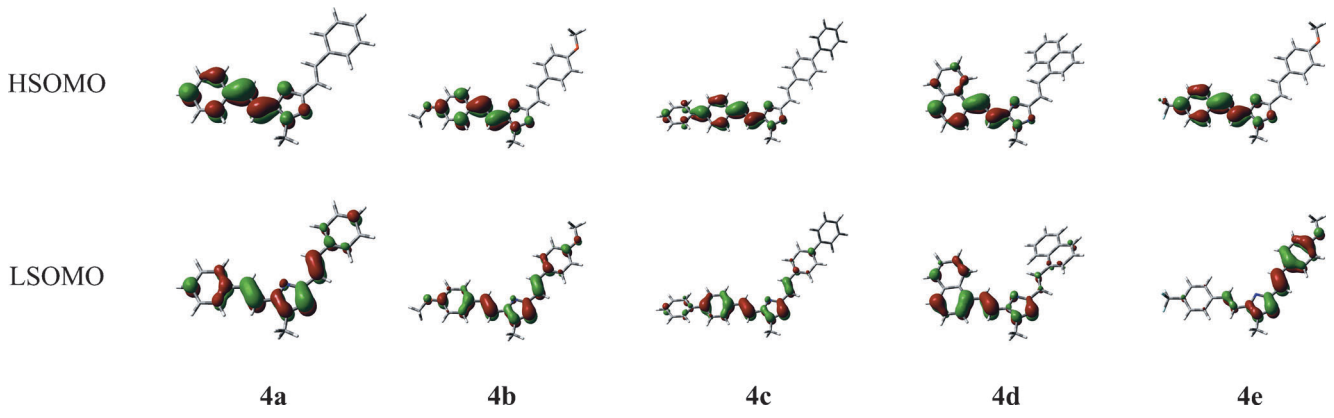

Figure 4. Isodensity singly occupied molecular orbitals (SOMOs) for **4a**–**e** in vacuum at the optimized S_1 geometry. Isodensity value: 0.04 e Bohr^{-3}.

pounds, as well as the short times required for completion of the reactions, make this approach particularly appealing as a sustainable synthetic protocol. The photophysical study revealed that alkenyl-1*H*-1,2,4-triazoles are promising blue-light-emitting dyes with high quantum yields up to 0.69. Moreover, it has been shown how the character of the emissive state depends on the substitution pattern of the 1*H*-1,2,4-triazole moiety. In this regard, the appropriate design of these derivatives can result in different levels of sensitivity to the environment, a characteristic that could find applications in many diverse areas. Compounds **4a**–**d**, which bear the same fragment on both the C-3 and C-5 positions, did not change their emission significantly regardless of the medium, whereas the emission from **4e** shifted as a function of the surrounding polarity. Finally, computational calculations satisfactorily supported the experimental results. The calculated condensed Fukui functions evidenced the markedly different electrophilicity of the carbon atoms of the 1*H*-1,2,4-triazole moiety, thereby explaining the difficulty in obtaining the dicoupled compounds in one synthetic step. Moreover, a very good estimation of the experimental fluorescence emission energies was obtained. More importantly, the computational protocol reported herein provides a cost-effective method for the prediction of fluorescence emissions in this class of compounds and it outperforms other more sophisticated, though more computationally expensive, calculations. As a result, a priori structure–emission relationships could be established for future fluorophores, thus minimizing the number of molecules to be synthesized and contributing to the overall sustainability of the process.

Experimental Section

Materials and solvents

Starting triazole **1** was prepared according to a published synthetic procedure.[30] Reagents were used as purchased except for phenylethyne and sodium iodide. Phenylethyne was distilled under reduced pressure prior to use. Sodium iodide was dried at 100 °C for 16 h under reduced pressure (0.5 Torr) and stored under argon atmosphere. All air-sensitive reactions were performed under argon atmosphere.

Synthesis and characterization

Microwave irradiations were performed in a Discover (CEM) focused microwave reactor. All the reactions were performed in the appropriate volume vessel with temperature monitoring using an IR pyrometer. Yields refer to isolated and purified products. Reactions were monitored by thin-layer chromatography performed on silica gel plates (60F-254) visualized under UV light. Column chromatography was performed on silica gel 60 (230–400 mesh). Melting points were determined on an SPM apparatus and are uncorrected. ^{1}H and ^{13}C NMR spectra were recorded on a Varian Unity 500 spectrometer. Chemical shifts (δ) are reported in parts per million (ppm) using Me_4Si as the internal reference and coupling constants (J) are given in Hertz. Multiplicities are denoted as follows: s = singlet, d = doublet, t = triplet, m = multiplet. MALDI-TOF mass spectra were measured on a Bruker Autoflex II TOF/TOF spectrometer (Bremen, Germany) using dithranol as the matrix. Samples co-crystallized with the matrix on the probe were ionized with a nitrogen laser pulse (337 nm) and accelerated under 20 kV with time-delayed extraction before entering the time-of-flight mass spectrometer. Matrix (10 mg mL^{-1}) and sample (1 mg mL^{-1}) were dissolved separately in methanol and mixed in a matrix/sample ratio ranging from 100:1 to 50:1. Typically, a mixture (5 μL) of matrix and sample was applied to a MALDI-TOF mass spectrometer probe and air-dried. MALDI-TOF mass spectrometry in positive reflector mode was used for all samples. External calibration was performed by using Peptide Calibration Standard II (covered mass range: 700–3200 Da), Protein Calibration Standard I (covered mass range: 5000–17 500 Da), and Protein Calibration Standard II (covered mass range: 20 000–70 000 Da) from Care (Bruker). The applied peak (m/z determination) detection method was the threshold centroid at 50% height of the peak maximum.

General procedure for C–C cross-coupling reactions

A mixture of tetrabutylammonium bromide (TBAB; 1 equiv), $Pd(OAc)_2$ (0.06 equiv), the appropriate aryltrimethoxysilane (**2**; 2 equiv), 3,5-dibromo-1-methyl-1*H*-1,2,4-triazole (**1**) or 5-arylalkenyl-3-bromo-1-methyl-1*H*-1,2,4-triazole (**3**) (1 equiv), and water (1 mL) was charged into a microwave vessel equipped with a magnetic stir bar. An aqueous solution of NaOH (50%) was added slowly and the resulting mixture was stirred vigorously. The vessel was closed and irradiated at 130 °C for 60 min. The crude reaction mixture was extracted with diethyl ether (5×10 mL) and the combined extracts were washed with 2 M NaOH (2×25 mL), 2 M HCl (30 mL), and brine (2×20 mL). The organic layer was dried ($MgSO_4$) and the solvent removed under reduced pressure. The residue was purified by chromatography, eluting with hexanes/ethyl acetate mixtures, to give analytically pure products **3** or **4**.

Compounds **3a**–**c**, **4a**, and **4b** were prepared according to this procedure and showed identical properties to those previously reported.[14]

(*E*)-3-Bromo-1-methyl-5-[2-(naphth-1-yl)vinyl]-1*H*-1,2,4-triazole (**3d**): Compound **1** (200 mg, 0.83 mmol) and (*E*)-triethoxy[2-(naphth-1-yl)-vinyl]silane (**2d**; 525 mg, 1.66 mmol), and employing hexanes/ethyl acetate (4:1) as the eluent, gave compound **3d** (201 mg, 77%) as a pale yellow solid. M.p. 116–117 °C; ^{1}H NMR ($CDCl_3$): δ = 8.55 (d, J = 15.4 Hz, 1H), 8.22 (d, J = 8.1 Hz, 1H), 7.89–7.86 (m, 2H), 7.75 (d, J = 8.1 Hz, 1H), 7.56–7.48 (m, 3H), 6.86 (d, J = 15.4 Hz, 1H), 3.91 ppm (s, 3H); ^{13}C NMR ($CDCl_3$): δ = 154.5, 139.2, 136.0, 133.6, 132.6, 131.3, 130.0, 128.6, 126.8, 126.3, 125.4, 124.1, 123.5, 112.1, 35.4 ppm; MS (MALDI-TOF): m/z calcd for $C_{15}H_{12}BrN_3$: 313.022; found: 314.030 $[M+H]^+$.

3,5-Bis[(*E*)-4-methoxystyryl]-1-methyl-1*H*-1,2,4-triazole (**4b**): Compound **3b** (150 mg, 0.51 mmol) and (*E*)-triethoxy(4-methoxystyryl)-silane (**2b**; 302 mg, 1.02 mmol), and employing hexanes/ethyl acetate (2:1) as the eluent, gave compound **4b** (171 mg, 93%) as a pale yellow solid. M.p. 152–153 °C; ^{1}H NMR ($CDCl_3$): δ = 7.74 (d, J = 15.7 Hz, 1H), 7.59 (d, J = 16.1 Hz, 1H), 7.54–7.49 (m, 4H), 6.95–6.90 (m, 5H), 6.76 (d, J = 16.1 Hz, 1H), 3.93 (s, 3H), 3.85 (s, 3H), 3.83 ppm (s, 3H); ^{13}C NMR ($CDCl_3$): δ = 160.7, 160.6, 159.8, 153.4, 137.2, 133.2, 129.3, 128.8, 128.8, 128.2, 115.3, 114.3, 114.1, 108.2, 55.3, 55.3, 35.1 ppm; MS (MALDI-TOF): m/z calcd for $C_{21}H_{21}N_3O_2$: 347.163; found: 348.139 $[M+H]^+$.

3,5-Bis{(*E*)-2-[(1,1′-biphenyl)-4-yl]vinyl}-1-methyl-1*H*-1,2,4-triazole (**4c**): Compound **3c** (174 mg, 0.51 mmol) and (*E*)-{2-[(1,1′-biphenyl)-4-yl]vinyl}triethoxysilane (**2c**; 349 mg, 1.02 mmol), and employing hexanes/ethyl acetate (4:1) as the eluent, gave compound **4c** (150 mg, 67%) as a pale yellow solid. M.p. 206–207 °C; ^{1}H NMR

($CDCl_3$): $\delta = 7.85$ (d, $J = 15.7$ Hz, 1H), 7.71–7.58 (m, 12H), 7.54–7.44 (m, 5H), 7.40–7.26 (m, 2H), 7.12 (d, $J = 16.1$ Hz, 1H), 6.96 (d, $J = 16.1$ Hz, 1H), 4.00 ppm (s, 3H); ^{13}C NMR ($CDCl_3$): $\delta = 160.9$, 153.5, 142.4, 141.3, 140.9, 140.5, 137.5, 135.8, 134.7, 133.5, 129.2, 129.1, 129.0, 128.1, 128.0, 127.8, 127.7, 127.6, 127.3, 127.2, 117.8, 110.7, 35.5 ppm; MS (MALDI-TOF): *m/z* calcd for $C_{31}H_{25}N_3$: 439.550; found: 440.213 $[M+H]^+$.

1-Methyl-3,5-bis[(*E*)-2-(naphth-1-yl)vinyl]-1*H*-1,2,4-triazole (**4d**): Compound **3d** (160 mg, 0.51 mmol) and (*E*)-triethoxy[2-(naphth-1-yl)vinyl]silane (**2d**; 323 mg, 1.02 mmol), and employing hexanes/ethyl acetate (4:1) as the eluent, gave compound **4d** (144 mg, 73%) as a pale yellow solid. M.p. 161–162 °C; ^1H NMR ($CDCl_3$): $\delta =$ 7.79 (d, $J = 16.1$ Hz, 1H), 7.64 (d, $J = 16.1$ Hz, 1H), 7.55–7.61 (m, 4H), 7.35–7.43 (m, 4H), 7.28–7.30 (m, 2H), 7.07 (d, $J = 16.1$ Hz, 1H), 6.90 (d, $J = 16.1$ Hz, 1H), 3.96 ppm (s, 3H); ^{13}C NMR ($CDCl_3$): $\delta = 160.8$, 153.3, 134.9, 134.1, 133.8, 133.7, 133.3, 131.4, 131.3, 130.8, 129.7, 128.7, 128.6, 126.7, 126.2, 126.1, 125.9, 125.7, 125.5, 124.1, 124.0, 123.9, 123.8, 120.5, 113.6, 35.3 ppm; MS (MALDI-TOF): *m/z* calcd for $C_{27}H_{21}N_3$: 387.174; found: 388.181 $[M+H]^+$.

Photophysical characterization

Absorption spectra were measured on a Varian Cary 5000 double-beam UV/Vis–near-IR spectrometer and were baseline corrected. Steady-state emission spectra of samples in solution in THF and 77 K glassy matrixes of 2-MeTHF were recorded on an Edinburgh FS920 spectrometer equipped with a 450 W xenon-arc lamp, excitation and emission monochromators (1.8 nm mm^{-1} dispersion; 1800 grooves mm^{-1} blazed at 500 nm), and a Hamamatsu R928 photomultiplier tube. Emission and excitation spectra were corrected for source intensity (lamp and grating) by standard correction curves. Steady-state emission spectra of solid samples were recorded on a HORIBA Jobin–Yvon IBHFL-322 Fluorolog 3 spectrometer equipped with a 450 W xenon-arc lamp, double-grating excitation and emission monochromators (2.1 nm mm^{-1} dispersion; 1200 grooves mm^{-1}), and a Hamamatsu R928 photomultiplier tube or a TBX-4-X single-photon-counting detector. Emission and excitation spectra were corrected for source intensity (lamp and grating) by standard correction curves. All time-resolved measurements were performed on an Edinburgh LifeSpec II instrument using the time-correlated single-photon-counting option. A 375 nm diode laser was used to excite the samples. The quality of the fit was assessed by minimizing the reduced χ^2 function and by visual inspection of the weighted residuals. Luminescence quantum yields were measured with a Hamamatsu Photonics absolute photoluminescence quantum yield (PLQY) measurement system (C9920–02) equipped with an L9799–01 continuous-wave xenon light source (150 W), monochromator, C7473 photonic multichannel analyzer, and integrating sphere, and employing U6039–05 PLQY measurement software (Hamamatsu Photonics, Ltd., Shizuoka, Japan). All solvents were spectrometric grade.

Computational details

All calculations were performed using the Gaussian 09[35] series of programs. Symmetry constraints were not considered in any calculation. Ground-state geometries were optimized with DFT[36] computations by using the parameter-free Perdew–Burke–Ernzerhof hybrid functional[37] and the standard Pople-style double-ζ basis set 6-31G*.[38] To simulate the absorption electronic spectrum down to 250 nm, for each compound the lowest 20–30 singlet ($S_0 \rightarrow S_n$) excitation energies were computed on the optimized geometry at S_0 by means of time-dependent density functional theory (TD-DFT)[22] calculations along with the 6-311+(2d,p) basis set. Oscillator strengths were deduced from the dipole transition-matrix elements. Excited-state geometries at S_1 were optimized using configuration interaction with all singly excited determinants (CIS)[21] with the 6-31G* basis set. To establish comparisons between the CIS-optimized excited-state geometries and the corresponding ground-state equilibrium geometries, the latter were recalculated with the HF method using 6-31G*. Geometries of compounds **4a** and **4e** at the S_1 level were additionally optimized at the TD-PBE0/6-31G* level of theory. Estimation of the fluorescence wavelengths was performed by considering the lowest vertical transition from TD-PBE0/6-311+G(2d,p) calculations at the S_1 optimized geometry. Solvent effects were introduced by using the polarizable continuum model (IEF-PCM)[39] with parameters for THF as implemented in Gaussian 09. The nature of all the stationary points was checked by computing vibrational frequencies, and all the species were found to be true potential energy minima, as no imaginary frequency was obtained (NImag = 0).

Acknowledgements

This study was supported by MINECO of Spain (project CTQ2011-22410) and Consejería de Educación y Ciencia JCCM (project PII2I09-0100). C.C. acknowledges MEC for an F.P.U. scholarship, and University of Castilla–La Mancha and the German Academic Exchange Service (DAAD) for financial support. Technical support from the High-Performance Computing Service of University of Castilla–La Mancha is gratefully acknowledged.

Keywords: density functional calculations · fluorescence · green chemistry · microwave chemistry · nitrogen heterocycles

[1] Some selected examples: a) A. Mishra, C.-Q. Ma, P. Bäuerle, *Chem. Rev.* **2009**, *109*, 1141–1276; b) B. E. Hardin, H. J. Snaith, M. D. McGehee, *Nature Photon.* **2012**, *6*, 162–169; c) M. Ethirajan, Y. Chen, P. Joshi, R. K. Pandey, *Chem. Soc. Rev.* **2011**, *40*, 340–362.

[2] A. Moulin, L. Demange, J. Ryan, D. Mousseaux, P. Sánchez, G. Bergé, D. Gagne, D. Perrissoud, V. Locatelli, A. Torsello, J. C. Galleyrand, J. A. Fehrentz, J. Martínez, *J. Med. Chem.* **2008**, *51*, 689–693.

[3] a) V. Thottempudi, H. Gao, J. M. Shreeve, *J. Am. Chem. Soc.* **2011**, *133*, 6464–6471; b) P. L. Wu, X. J. Feng, H. L. Tam, M. S. Wong, K. W. Cheah, *J. Am. Chem. Soc.* **2009**, *131*, 886–887.

[4] F. Liu, X. Bugaut, M. Schedler, R. Fröhlich, F. Glorius, *Angew. Chem.* **2011**, *123*, 12834–12839; *Angew. Chem. Int. Ed.* **2011**, *50*, 12626–12630.

[5] Some selected examples: a) S. J. Yeh, W.-C. Wu, C.-T. Chen, Y.-H. Song, Y. Chi, M.-H. Ho, S.-F. Hsu, C.-H. Chen, *Adv. Mater.* **2005**, *17*, 285–289; b) E. Orselli, G. S. Kottas, A. E. Konradsson, P. Coppo, R. Fröhlich, L. De Cola, A. van Dijken, M. Büchel, H. Börner, *Inorg. Chem.* **2007**, *46*, 11082–11093; c) M. Mydlak, M. Mauro, F. Polo, M. Felicetti, J. Leonhardt, G. Diener, L. De Cola, C. A. Strassert, *Chem. Mater.* **2011**, *23*, 3659–3667; d) S. Kume, K. Kuroiwa, N. Kimizuka, *Chem. Commun.* **2006**, 2442–2444; e) S. Fanni, T. E. Keyes, C. M. O'Connor, H. Hughes, R. Wang, J. G. Vos, *Coord. Chem. Rev.* **2000**, *208*, 77–86.

[6] Some selected examples: a) J. G. Haasnoot, *Coord. Chem. Rev.* **2000**, *200–202*, 131–185; b) G. Aromí, L. A. Barrios, O. Roubeau, P. Gamez, *Coord. Chem. Rev.* **2011**, *255*, 485–546; c) K. Liu, W. Shi, P. Cheng, *Dalton Trans.* **2011**, *40*, 8475–8490; d) Z. Xu, Q. Wang, H. Li, W. Meng, Y. Han, H. Hou, Y. Fan, *Chem. Commun.* **2012**, *48*, 5736–5738.

[7] Some selected examples: a) L.-S. Yu, S.-A. Chen, *Adv. Mater.* **2004**, *16*, 744–748; b) T. Yasuda, K. Namekawa, T. Iijima, T. Yamamoto, *Polymer* **2007**, *48*, 4375–4384; c) C.-S. Wu, Y. Chen, *J. Mater. Chem.* **2010**, *20*, 7700–7709; d) F. Montilla, F. Huerta, D. Salinas-Torres, E. Morallón, C. Cebrián, P. Prieto, Á. Díaz-Ortiz, A. de La Hoz, J. R. Carrillo, C. Romero,

Electrochim. Acta **2011**, *58*, 215 – 222; e) B. Campagne, G. David, B. Améduri, D. J. Jones, J. Rozière, I. Roche, *Macromolecules* **2013**, *46*, 3046 – 3057.

[8] L.-R. Tsai, Y. Chen, *Macromolecules* **2007**, *40*, 2984 – 2992.

[9] a) R. R. Kayumova, S. S. Ostakhov, A. V. Mamykin, R. R. Muslukhov, G. F. Iskhakova, S. P. Ivanov, S. A. Meshcheryakova, E. E. Klen, F. A. Khaliullin, V. P. Kazakov, *Russ. J. Gen. Chem.* **2011**, *81*, 1203 – 1210; b) D. Cáceres, C. Cebrián, A. M. Rodríguez, J. R. Carrillo, Á. Díaz-Ortiz, P. Prieto, F. Aparicio, F. García, L. Sánchez, *Chem. Commun.* **2013**, *49*, 621 – 623.

[10] Some selected examples: a) S. Ueda, H. Nagasawa, *J. Am. Chem. Soc.* **2009**, *131*, 15080 – 15081; b) R. Hage, R. Prins, J. G. Haasnoot, J. Reedijk, J. G. Vos, *J. Chem. Soc. Dalton Trans.* **1987**, 1389 – 1395; c) V. F. Ferreira, D. R. Da Rocha, F. C. Da Silva, P. G. Ferreira, N. A. Boechat, J. L. Magalhães, *Expert Opin. Ther. Pat.* **2013**, *23*, 319 – 331; d) J. Sharma, S. Ahmad, M. Shamsher Alam, *J. Chem. Pharm. Res.* **2012**, *4*, 5157 – 5164; e) S. C. Holm, B. F. Straub, *Org. Prep. Proced. Int.* **2011**, *43*, 319 – 347; f) J. Košmrlj, M. Kočevar, S. Polanc, *Synlett* **2009**, 2217 – 2235; g) I. A. Al-Masoudi, Y. A. Al-Soud, N. J. Al-Salihi, N. A. Al-Masoudi, *Chem. Heterocycl. Chem.* **2006**, *42*, 1377 – 1403; h) E. S. H. El Ashry, N. Rashed, *Curr. Org. Chem.* **2000**, *4*, 609 – 651.

[11] S. Libnow, S. Wille, A. Christiansen, M. Hein, H. Reinke, M. Köckerling, R. Miethchen, *Synthesis* **2006**, 496 – 508.

[12] a) S. Wille, M. Hein, R. Miethchen, *Tetrahedron* **2006**, *62*, 3301 – 3308; b) I. N. Houpis, R. Liu, Y. Wu, Y. Yuan, Y. Wang, U. Nettekoven, *J. Org. Chem.* **2010**, *75*, 6965 – 6968; c) S. Katkevica, P. Salun, A. Jirgensons, *Tetrahedron Lett.* **2013**, *54*, 4524 – 4525.

[13] C. Cebrián, A. de Cózar, P. Prieto, A. Díaz-Ortiz, A. de La Hoz, J. R. Carrillo, A. M. Rodríguez, F. Montilla, *Synlett* **2010**, 55 – 60.

[14] A. Díaz-Ortiz, P. Prieto, A. de Cózar, C. Cebrián, A. Moreno, A. de La Hoz, *Aust. J. Chem.* **2009**, *62*, 1600 – 1606.

[15] C. Tubaro, A. Biffis, E. Scattolin, M. Basato, *Tetrahedron* **2008**, *64*, 4187 – 4195.

[16] a) P. T. Anastas, J. C. Warner, *Green Chemistry Theory and Practice*, Oxford University Press, New York, **1988**; b) P. T. Anastas, T. C. Williamson, in *Green Chemistry Frontiers in Benign Chemical Synthesis and Processes*, Oxford University Press, New York, **1988**.

[17] P. Anastas, N. Eghbali, *Chem. Soc. Rev.* **2010**, *39*, 301 – 312.

[18] a) L. L. Shi, T. Li, S. S. Zhao, H. Li, Z. Su, *Theor. Chem. Acc.* **2009**, *124*, 29 – 36; b) A. Brown, T. Y. Ngai, M. A. Barnes, J. A. Key, C. W. Cairo, *J. Phys. Chem. A* **2012**, *116*, 46 – 54.

[19] M. D. Halls, H. B. Schlegel, *Chem. Mater.* **2001**, *13*, 2632 – 2640.

[20] D. Jacquemin, E. A. Perpète, G. Scalmani, M. J. Frisch, I. Ciofini, C. Adamo, *Chem. Phys. Lett.* **2006**, *421*, 272 – 276.

[21] J. B. Foresman, M. Head-Gordon, J. A. Pople, M. J. Frisch, *J. Phys. Chem.* **1992**, *96*, 135 – 149.

[22] a) E. Runge, E. K. U. Gross, *Phys. Rev. Lett.* **1984**, *52*, 997 – 1000; b) M. E. Casida, C. Jamorski, K. C. Casida, D. R. Salahub, *J. Chem. Phys.* **1998**, *108*, 4439 – 4449; c) K. Burke, J. Werschnik, E. K. Gross, *J. Chem. Phys.* **2005**, *123*, 062206 – 062214; d) F. Furche, D. Rappaport in *Computational Photochemistry, Vol. 16* (Ed.: M. Olivucci), Elsevier, Amsterdam, **2005**, Chapter 3.

[23] a) L. Yang, J.-K. Feng, A.-M. Ren, J.-Z. Sun, *Polymer* **2006**, *47*, 1397 – 1404; b) R. de Vivie-Riedle, V. De Waele, L. Kurtz, E. Riedle, *J. Phys. Chem. A* **2003**, *107*, 10591 – 10599; c) B.-Z. Yang, X. Zhou, T. Liu, F.-Q. Bai, H.-X. Zhang, *Int. J. Quantum Chem.* **2011**, *111*, 2258 – 2267.

[24] a) A. de La Hoz, A. Díaz-Ortiz, A. Moreno, *Curr. Org. Chem.* **2004**, *8*, 903 – 918; b) A. de La Hoz, A. Díaz-Ortiz, A. Moreno, *Chem. Soc. Rev.* **2005**, *34*, 164 – 178; c) F. G. Brunetti, M. A. Herrero, J. de M. Muñoz, A. Díaz-Ortiz, J. Alfonsi, M. Meneghetti, M. Prato, E. Vazquez, *J. Am. Chem. Soc.* **2008**, *130*, 8094 – 8100; d) N. Rubio, M. A. Herrero, M. Meneghetti, A. Díaz-Ortiz, M. Schiavon, M. Prato, E. Vázquez, *J. Mater. Chem.* **2009**, *19*, 4407 – 4413; e) M. Moral, A. Ruiz, A. Moreno, A. Díaz-Ortiz, I. López-Solera, A. de La Hoz, A. Sánchez-Migallón, *Tetrahedron* **2010**, *66*, 121 – 127; f) A. de La Hoz, A. Díaz-Ortiz, A. Sánchez Migallón, M. V. Gómez Almagro, P. Prieto in *Microwaves in Organic Synthesis. Third Edition* (Eds.: A. de La Hoz, A. Loupy), Wiley-VCH, Weinheim, **2012**, pp. 245 – 295.

[25] a) A. de La Hoz, P. Prieto, M. Rajzmann, A. de Cózar, A. Díaz-Ortiz, A. Moreno, F. P. Cossío, *Tetrahedron* **2008**, *64*, 8169 – 8176; b) M. V. Gómez, A. I. Aranda, A. Moreno, F. P. Cossío, A. de Cózar, A. Díaz-Ortiz, A. de La Hoz, P. Prieto, *Tetrahedron* **2009**, *65*, 5328 – 5336; c) A. de Cózar, M. C. Millán, C. Cebrián, P. Prieto, A. Díaz-Ortiz, A. de La Hoz, *Org. Biomol. Chem.* **2010**, *8*, 1000 – 1009; d) A. M. Rodriguez, C. Cebrián, P. Prieto, J. I. García, A. de La Hoz, Á. Díaz-Ortiz, *Chem. Eur. J.* **2012**, *18*, 6217 – 6224.

[26] a) Y. Hatanaka, T. Hiyama, *J. Org. Chem.* **1988**, *53*, 918 – 920; b) Y. Hatanaka, K. Goda, T. Hiyama, *J. Organomet. Chem.* **1994**, *465*, 97 – 100; c) T. Hiyama, *J. Organomet. Chem.* **2002**, *653*, 58 – 61.

[27] S. E. Denmark, M. H. Ober, *Aldrichimica Acta* **2003**, *36*, 75 – 85.

[28] Some selected examples: a) T. Hiyama, E. Shirakawa, *Top. Curr. Chem.* **2002**, *219*, 61 – 85; b) M. L. Clarke, *Adv. Synth. Catal.* **2005**, *347*, 303 – 307; c) C. J. Handy, A. S. Manoso, W. T. McElroy, W. M. Seganish, P. DeShong, *Tetrahedron* **2005**, *61*, 12201 – 12225; d) E. Alacid, C. Nájera, *Adv. Synth. Catal.* **2006**, *348*, 945 – 952; e) E. Alacid, C. Nájera, *J. Org. Chem.* **2008**, *73*, 2315 – 2322; f) S. Napier, S. M. Marcuccio, H. Tye, M. Whittaker, *Tetrahedron Lett.* **2008**, *49*, 3939 – 3942; g) E. J. Milton, J. A. Fuentes, M. L. Clarke, *Org. Biomol. Chem.* **2009**, *7*, 2645 – 2648; h) I. Peñafiel, I. M. Pastor, M. Yus, *Eur. J. Org. Chem.* **2013**, 1479 – 1484.

[29] a) E. T. Iamazaki, T. D. Z. Atvars, *Langmuir* **2006**, *22*, 9866 – 9873; b) W. H. Melhuish, *J. Phys. Chem.* **1961**, *65*, 229 – 235.

[30] A. Zumbrunn, *Synthesis* **1998**, 1357 – 1361.

[31] a) C. Y. Legault, Y. Garcia, C. A. Merlic, K. N. Houk, *J. Am. Chem. Soc.* **2007**, *129*, 12664 – 12665; b) Y. Garcia, F. Schoenebeck, C. Y. Legault, C. A. Merlic, K. N. Houk, *J. Am. Chem. Soc.* **2009**, *131*, 6632 – 6639.

[32] R. G. Parr, W. Yang, *Density-Functional Theory of Atoms and Molecules*, Oxford University Press, New York, **1989**.

[33] a) W. Yang, W. J. Mortier, *J. Am. Chem. Soc.* **1986**, *108*, 5708 – 5711; b) The values of the localized Fukui function were evaluated taking into account orbital relaxation: P. W. Ayers, M. Levy, *Theor. Chem. Acc.* **2000**, *103*, 353 – 360.

[34] The use of the range-separated hybrid functional CAM-B3LYP, which has proven useful in studying systems exhibiting charge-transfer excited states, either for the vertical transition $S_0 \leftarrow S_1$ or for both S_1 optimization and subsequent vertical transition $S_0 \leftarrow S_1$, provided estimated emission energies of 3.27 and 3.11 eV, respectively.

[35] Gaussian 09, Revision A.1, M. J. Frisch, G. W. Trucks, H. B. Schlegel, G. E. Scuseria, M. A. Robb, J. R. Cheeseman, G. Scalmani, V. Barone, B. Mennucci, G. A. Petersson, H. Nakatsuji, M. Caricato, X. Li, H. P. Hratchian, A. F. Izmaylov, J. Bloino, G. Zheng, J. L. Sonnenberg, M. Hada, M. Ehara, K. Toyota, R. Fukuda, J. Hasegawa, M. Ishida, T. Nakajima, Y. Honda, O. Kitao, H. Nakai, T. Vreven, J. A. Montgomery, Jr., J. E. Peralta, F. Ogliaro, M. Bearpark, J. J. Heyd, E. Brothers, K. N. Kudin, V. N. Staroverov, R. Kobayashi, J. Normand, K. Raghavachari, A. Rendell, J. C. Burant, S. S. Iyengar, J. Tomasi, M. Cossi, N. Rega, J. M. Millam, M. Klene, J. E. Knox, J. B. Cross, V. Bakken, C. Adamo, J. Jaramillo, R. Gomperts, R. E. Stratmann, O. Yazyev, A. J. Austin, R. Cammi, C. Pomelli, J. W. Ochterski, R. L. Martin, K. Morokuma, V. G. Zakrzewski, G. A. Voth, P. Salvador, J. J. Dannenberg, S. Dapprich, A. D. Daniels, Farkas, J. B. Foresman, J. V. Ortiz, J. Cioslowski, D. J. Fox, Gaussian, Inc., Wallingford CT, **2009**.

[36] R. G. Parr, W. Yang, *Density Functional Theory of Atoms and Molecules*, Oxford University Press, New York, **1994**.

[37] a) J. P. Perdew, K. Burke, M. Ernzerhof, *Phys. Rev. Lett.* **1996**, *77*, 3865 – 3868; b) J. P. Perdew, K. Burke, M. Ernzerhof, *Phys. Rev. Lett.* **1997**, *78*, 1396; c) C. Adamo, V. Barone, *J. Chem. Phys.* **1999**, *110*, 6158 – 6170.

[38] a) R. Ditchfield, W. J. Hehre, J. A. Pople, *J. Chem. Phys.* **1971**, *54*, 724 – 728; b) W. J. Hehre, R. Ditchfield, J. A. Pople, *J. Chem. Phys.* **1972**, *56*, 2257 – 2261; c) P. C. Hariharan, J. A. Pople, *Theor. Chim. Acta* **1973**, *28*, 213 – 222; d) P. C. Hariharan, J. A. Pople, *Mol. Phys.* **1974**, *27*, 209 – 214.

[39] a) E. Cancès, B. Mennucci, J. Tomasi, *J. Chem. Phys.* **1997**, *107*, 3032 – 3041; b) M. Cossi, G. Scalmani, N. Rega, V. Barone, *J. Chem. Phys.* **2002**, *117*, 43 – 54.

Received: May 26, 2014
Published online on July 23, 2014